

# Graded synaptic transmission at the *Caenorhabditis elegans* neuromuscular junction

Qiang Liu, Gunther Hollopeter, and Erik M. Jorgensen<sup>1</sup>

Department of Biology and Howard Hughes Medical Institute, University of Utah, Salt Lake City, UT 84112-0840

Edited by Cornelia I. Bargmann, Rockefeller University, New York, NY, and approved April 27, 2009 (received for review April 2, 2009)

**Most neurotransmission is mediated by action potentials, whereas sensory neurons propagate electrical signals passively and release neurotransmitter in a graded manner. Here, we demonstrate that *Caenorhabditis elegans* neuromuscular junctions release neurotransmitter in a graded fashion. When motor neurons were depolarized by light-activation of channelrhodopsin-2, the evoked postsynaptic current scaled with the strength of the stimulation. When motor neurons were hyperpolarized by light-activation of halorhodopsin, tonic release of synaptic vesicles was decreased. These data suggest that both evoked and tonic neurotransmitter release is graded in response to membrane potential. Acetylcholine synapses are depressed by high-frequency stimulation, in part due to desensitization of the nicotine-sensitive ACR-16 receptor. By contrast, GABA synapses facilitate before becoming depressed. Graded transmission and plasticity confer a broad dynamic range to these synapses. Graded release precisely transmits stimulation intensity, even hyperpolarizing inputs. Synaptic plasticity alters the balance of excitatory and inhibitory inputs into the muscle in a use-dependent manner.**

channelrhodopsin-2 | graded release | halorhodopsin | synaptic depression | synaptic facilitation

In most neurons, propagation of an electrical signal occurs via all-or-none action potentials. These regenerative depolarizations ensure that signal transmission is robust and reliable over long distances. Conversely, some neurons lack action potentials, and rely instead on passive propagation and graded release of neurotransmitter. Graded synaptic transmission depends on two attributes: passive propagation of membrane depolarization along the axon, and non-saturating calcium influx at the synaptic bouton. Thus, graded transmission is associated with a paucity or absence of the voltage-gated ion channels in the axon, and incomplete activation of voltage-gated calcium channels at the synapse. Graded release of neurotransmitter underlies synaptic transmission in spiking neurons as well: if action potentials are blocked by tetrodotoxin neurotransmitter, release varies linearly with membrane potential (1, 2). The action potential simply fixes the size of the depolarization of the bouton.

The most well studied graded synapses are the ribbon synapses of the vertebrate retina, either those of the photoreceptor or the bipolar cells (3). These neurons exhibit tonic release of neurotransmitter at rest. Evoked responses scale with the presynaptic stimulus (4) and thereby increase the information content at synapses. Sustained depolarization of the presynaptic cell results in increased neurotransmitter release (presumably by increasing miniature postsynaptic currents), and hyperpolarization results in decreased neurotransmitter release. These synapses show marked depression when stimulated but are also capable of high levels of sustained transmission under continuous stimulation (5, 6).

It has long been believed that nematodes rely largely on passive propagation rather than action potentials. Early studies by del Castillo and colleagues hinted that neuromuscular junctions from the parasitic nematode *Ascaris suum* may exhibit graded release of acetylcholine (7). Incontrovertible evidence for graded release in *Ascaris* was obtained by Davis and Stretton (8,9). Neurotransmitter release from the motor neurons is tonic (8). These motor neurons exhibit linear changes in membrane potential in response to injected

currents (9), and depolarization is passively propagated to synaptic regions. However, the *Ascaris* muscles are too large to accommodate voltage-clamp studies, so miniature postsynaptic currents were never recorded. Presumably changes in the membrane potential of the motor neuron result in graded synaptic vesicle exocytosis, but this has not been demonstrated.

Indirect evidence suggests that the nematode *Caenorhabditis elegans* also relies on passive propagation. Classical voltage-gated sodium channels are absent in the *C. elegans* genome (10). Consistent with this observation, the first electrophysiological recordings from *C. elegans* neurons demonstrated that the ASE sensory neuron is isopotential and lacks classical sodium-driven action potentials (11). A more recent study found that the AVA command interneuron also lacks action potentials, although certain neurons such as the motor neuron RMD exhibit calcium-dependent voltage-gated plateau potentials, suggesting that all-or-nothing signaling exists in *C. elegans* (12). Thus, it appears that both analog coding and digital coding schemes exist in the *C. elegans* nervous system (13). It is not known whether the motor neurons in *C. elegans* act in a phasic or graded fashion. Here, we perform voltage-clamp analysis of the body muscles and find that the postsynaptic response scales with the strength of the stimulus to the motor neurons.

Typically, motor neurons in *C. elegans* are depolarized by applying an electric field to the bundle of axons in the ventral nerve cord. As an alternative to field stimulation, motor neurons can be selectively activated using the light-activated ion channel channelrhodopsin-2 (hereafter referred to as channelrhodopsin) (14). Channelrhodopsin is a 7-pass trans-membrane protein from the green algae *Chlamydomonas reinhardtii* (15), and forms a cation channel activated by blue light. This channel can be heterologously expressed and thereby confer excitation by light in many cells including *Xenopus* oocytes, HEK293 cells, mammalian central neurons, as well as *C. elegans* muscles and neurons (14–19). In all these systems, channelrhodopsin expression results in rapid depolarizing currents upon light stimulation, and it can be used for selective activation. Conventional field stimulation in *C. elegans* have been limited to single or low-frequency stimuli (20, 21), as it is likely that repetitive stimulation kills the motor neurons. By contrast, motor neurons can tolerate high-frequency stimulation by channelrhodopsin (14). Thus, channelrhodopsin offers an improved method for stimulation of the *C. elegans* neuromuscular junction compared with electrical stimulation.

## Results

**Fast-Activating Photocurrents in *C. elegans* Muscles.** The optimized version of channelrhodopsin (H134R, C-terminal deletion) (18) was fused to the red fluorescent mCherry protein (ChR2::mCherry). This fusion protein was expressed under the control of the muscle-

Author contributions: Q.L. and E.M.J. designed research; Q.L. performed research; G.H. contributed new reagents/analytic tools; Q.L. analyzed data; and Q.L., G.H., and E.M.J. wrote the paper.

The authors declare no conflict of interest.

This article is a PNAS Direct Submission.

To whom correspondence should be addressed. E-mail: jorgensen@biology.utah.edu.

This article contains supporting information online at [www.pnas.org/cgi/content/full/0903570106/DCSupplemental](http://www.pnas.org/cgi/content/full/0903570106/DCSupplemental).

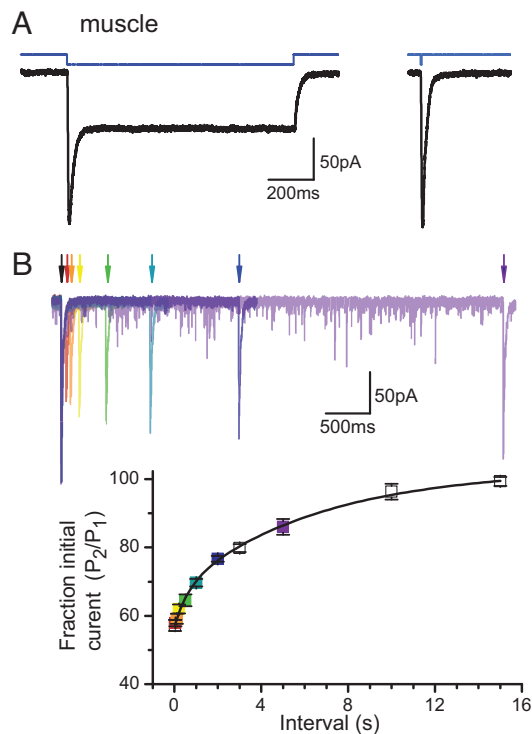


**Fig. 1.** Channelrhodopsin-induced photocurrents in muscle. (A) Photocurrents activated by a 1 s (Left) or 3 ms (Right) light pulse. The downward deflection of the blue line indicates that blue light is on. (B) Paired-pulse analysis of channelrhodopsin recovery from the steady state. (Top) Seven overlaid photocurrent traces activated by pairs of 3-ms light pulses with intervals of 50 ms, 100 ms, 200 ms, 500 ms, 1 s, 2 s, and 5 s. All traces were aligned to the first light pulse (black arrow). The second pulses are indicated by colored arrows. (Bottom) Ratio of the second to the first peak was plotted against paired-pulse intervals. The recovery curve was best fit by a double-exponential function ( $\tau_{\text{fast}} = 0.6 \text{ s} \pm 0.5$ ,  $\tau_{\text{slow}} = 6.4 \text{ s} \pm 3.2$ ,  $n = 6$ ).

specific *myo-3* promoter (*Pmyo-3::ChR2::mCherry*) in *C. elegans* and integrated into a chromosome [supporting information (SI) Fig. S1A]. When the strain was raised in the presence of all-trans retinal, contraction of the body muscles in these animals was observed upon exposure to blue light (data not shown). A 1-second light stimulus triggered an inward photocurrent that rapidly declined to a steady state at approximately 50% of the initial current (Fig. 1A Left). Currents with similar peak amplitude were elicited by 3-ms stimuli (Fig. 1A Right).

To determine the temporal resolution of channelrhodopsin-mediated photocurrents, we applied a train of 3-ms light pulses at increasing stimulation frequencies. At frequencies of 1, 5, and 10 Hz, channelrhodopsin was able to fully close during inter-pulse periods of darkness (Fig. S2). At 20 Hz stimulation, photocurrents no longer returned to baseline during the inter-pulse period, resulting in an elevated basal current component throughout the train (Fig. S2). Therefore, the maximal stimulation rate is 20 Hz for 3-ms light pulses. At all stimulation frequencies tested, the first peak of the train was similar in amplitude, and subsequent light-induced currents rapidly decreased in peak amplitude. Under high-frequency stimulation, the peak responses subsided to a level that was similar to the steady-state current attained upon prolonged light exposure. More than half of the initial current remains, and these trains of transients can be sustained for many seconds, suggesting that channelrhodopsin is not down-regulated by slow forms of inactivation, such as endocytosis, for the duration of these stimulations.

To determine the recovery rate of channelrhodopsin from the

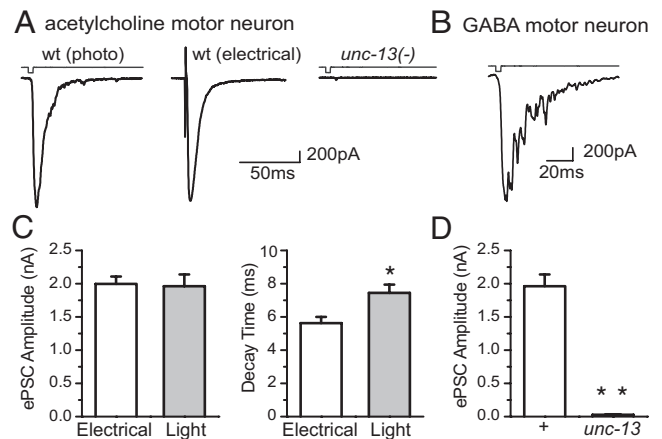


**Fig. 2.** Light-activated postsynaptic currents. (A) (Left) Acetylcholine postsynaptic current evoked by a 3-ms light pulse (*Punc-17::ChR2::mCherry*). (Middle) Electrically evoked current from the WT. (Right) A 3-ms light pulse failed to evoke postsynaptic response in *unc-13(s69) Punc-17::ChR2::mCherry*. (B) GABA postsynaptic current evoked by a 3-ms light pulse (*Punc-47::ChR2::mCherry*). (C) Comparison of amplitude (Left) and decay time (Right) between light-evoked (gray column,  $n = 9$ ) and electrically evoked (white column,  $n = 16$ ) postsynaptic currents. (Electrical:  $2.01 \text{ nA} \pm 0.11$ ,  $\tau_{\text{decay}} = 5.6 \text{ ms} \pm 0.4$ ; light:  $1.96 \text{ nA} \pm 0.18$ ,  $\tau_{\text{decay}} = 7.4 \text{ ms} \pm 0.5$ ;  $*P < 0.01$ , 2-sample *t* test). (D) UNC-13 is required for light-evoked postsynaptic currents ( $0.03 \text{ nA} \pm 0.01$ ,  $n = 5$ ,  $**P < 0.00001$ , 2-sample *t* test).

steady state, we performed a series of paired-pulse trials (Fig. 1B). We determined the ratio of the second peak to the first peak, and plotted these ratios relative to the recovery intervals (Fig. 1B Bottom). This recovery curve was best fit by a double-exponential function with time constants of  $6.4 \text{ s} \pm 3.2$  and  $0.6 \text{ s} \pm 0.5$ . The slow component of recovery is similar to reports of channelrhodopsin currents in HEK cells (6.4 s) (18), rat hippocampus neurons (5.1 s) (16), and yeast cells (8 s) (22), and likely represents the time required for retinal to re-isomerize back to the all-trans ground state. The fast recovery component has not been reported before, probably because previous studies did not examine paired pulses with intervals  $< 1 \text{ s}$ . Nevertheless, the 0.6-s fast recovery time falls in the range of transition time from the inactivated state to the closed state (60 ms to  $\approx 2 \text{ s}$ ) in the 3-state photo cycle modeling of channelrhodopsin (15).

**Light-Activated Motor Neurons.** We expressed channelrhodopsin in acetylcholine neurons using the *unc-17* promoter (*Punc-17::ChR2::mCherry*). The expression of channelrhodopsin was confirmed by the presence of red fluorescence in the cell bodies of acetylcholine neurons (Fig. S1B). These currents were completely blocked by *d*-tubocurarine (data not shown), demonstrating that it was caused by acetylcholine release. The current amplitudes induced by light activation of the motor neurons resemble those evoked by electrical stimulation (Fig. 2A), although decay kinetics were slightly slower (Fig. 2C;  $P < 0.01$ ). To confirm that light-evoked currents result from the canonical synaptic vesicle fusion machinery, we tested whether these currents required the *unc-13* gene. UNC-13 is a protein essential for synaptic vesicle exocytosis (23–25). Consistent with the absence of electrically evoked currents in *unc-13(s69)* mutants (25), light stimuli failed to evoke detectable currents in *unc-13(s69) Punc-17::ChR2::mCherry* animals (Fig. 2A and D).

In contrast to acetylcholine motor neurons, evoked currents are not observed in GABA motor neurons with stimulating electrodes (26, 27), possibly because they lack long processes in the ventral cord (Fig. S3). To evoke GABA release by using light, we selectively expressed channelrhodopsin in GABA neurons using the *unc-47* promoter. Transgenic worms were verified by the presence of red fluorescence in the nerve cord (Fig. S1C). Animals were dissected

and the muscles voltage-clamped at  $-60\text{mV}$ ; blue light evoked robust postsynaptic currents (Fig. 2*B*). This current was not reduced by the presence of *d*-tubocurarine (data not shown), demonstrating that it was not caused by acetylcholine release. Compared with light-evoked acetylcholine currents, GABA currents were slightly smaller in amplitude ( $1.23\text{ nA} \pm 0.12$ ,  $n = 13$ ) and slower in decay time ( $24.8\text{ ms} \pm 2.7$ ,  $n = 12$ ), and were accompanied by profound asynchronous release (Fig. 2*B*).

**C. *elegans* Neuromuscular Junctions Exhibit Graded Release.** We used light stimulation to determine if motor neurons exhibit graded release. If synaptic currents are stimulated by an action potential, presynaptic photocurrents that exceed the threshold should trigger postsynaptic currents of the same amplitude. Conversely, if synaptic currents are caused by graded release, increasing the strength of the stimulus will result in a gradual increase in the postsynaptic current. To differentiate between these 2 possibilities, we varied the intensity of the light stimulus to the acetylcholine motor neurons (in *Punc-17::ChR2::mCherry*) using a fixed stimulation period (3 ms light pulse). The postsynaptic currents increased monotonically with increasing light stimuli to the motor neurons (Fig. 3*A*). Similarly, photocurrents induced directly in the muscle (in *Pmyo-3::ChR2::mCherry*) increased monotonically with increasing light stimuli. We compared postsynaptic currents to photocurrents in the muscle stimulated by the same light intensity. Both directly induced photocurrents and evoked postsynaptic currents increased monotonically as the light intensity was increased (Fig. 3*B*). After normalizing to the current amplitudes induced by our maximum illumination intensity ( $\approx 10\text{ mW/mm}^2$ ), the photocurrents and evoked postsynaptic responses coincided and were directly proportional (Fig. 3*B* and *C*). In short, graded presynaptic depolarization of the motor neurons by photo-stimulation elicits graded postsynaptic currents.

Many graded synapses release neurotransmitter tonically, such that hyperpolarization reduces neurotransmitter release and depolarization increases neurotransmitter release (8). One possible mechanism that has been put forward for graded release is that the resting membrane potential of the neuron might lie in the middle of the activation curve of the voltage-gated calcium channel, so that small changes in the membrane potential could lead to increases or decreases in calcium influx (28). This model suggests that the mini frequencies should decrease if the motor neuron is hyperpolarized. A potential technique for introducing hyperpolarization is by expressing halorhodopsin in the motor neurons. Halorhodopsin is a light-activated chloride pump; chloride transport into the cell will hyperpolarize excitable cells and decrease their activity (17, 19). We generated a construct in which the halorhodopsin was fused to GFP (*Halo::GFP*) and expressed this fusion protein in acetylcholine motor neurons under the control of the *unc-17* promoter (*Punc-17::Halo::GFP*). Exposure to yellow light paralyzed the transgenic animals raised in the presence of all-trans retinal (data not shown). Endogenous acetylcholine miniature currents were recorded at the neuromuscular junction of halorhodopsin-expressing worms. The recording pipette solutions were adjusted so that chloride was at equilibrium at the  $-60\text{-mV}$  holding potential and thereby eliminating confounding currents from the GABA neurons. The frequency of minis was significantly decreased during a 5-s flash of yellow light (Fig. 3*D* and *E*), suggesting that *C. elegans* acetylcholine motor neurons tonically release neurotransmitter at resting membrane potential and this release is at a dynamic range that can be either up- or down-regulated by membrane potential. Interestingly, the frequency of minis increased immediately after the light pulse (Fig. 3*E*). Amplitudes of minis did not change during or after the light stimulation, indicating that the properties of postsynaptic receptors were not altered.

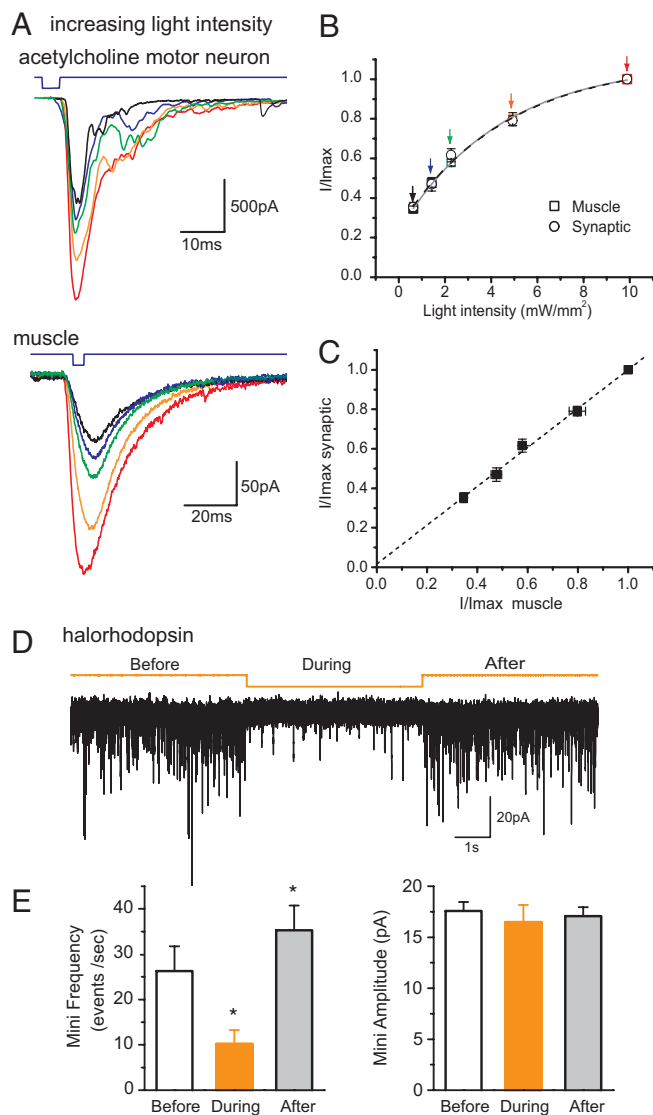


**Fig. 3.** Graded acetylcholine release. (A) Photocurrents from muscle and postsynaptic currents from acetylcholine synapses evoked by blue light at variable intensities (*Punc-17::ChR2::mCherry*). Light intensities ( $\text{mW/mm}^2$ ): red, 9.9; orange, 4.9; green, 2.3; blue, 1.4; black, 0.6. (B) Muscle photocurrents (square) and acetylcholine postsynaptic currents (circle) were normalized to their maximum amplitudes and plotted with light intensity. The normalized muscle and postsynaptic curves each were fitted with a single exponent and overlapped. Color arrows are corresponding to light intensities used in A. (C) Normalized postsynaptic currents are directly proportional to normalized muscle photocurrents. (D) Endogenous acetylcholine release recorded from *Punc-17::Halo::GFP* before, during, and after illumination. The downward deflection of the yellow line indicates that the yellow light is on. (E) Statistical comparison of mini frequency and amplitude before, during, and after light pulse. Mini frequencies: before (white column),  $26.3 \pm 5.4$ ; during (yellow column),  $10.2 \pm 3.1$ ; and after (gray column),  $35.3 \pm 5.5$  (events/s). Mini amplitudes: before,  $17.6\text{ pA} \pm 0.9$ ; during,  $16.5\text{ pA} \pm 1.7$ ; after,  $17.1\text{ pA} \pm 0.9$ . \* $P < 0.01$ , 1-way ANOVA,  $n = 5$ .

#### Depression Versus Facilitation at Acetylcholine and GABA Synapses.

We subjected acetylcholine and GABA motor neurons to repetitive stimulation to observe synaptic plasticity. At all stimulation frequencies tested, even at as low as 1 Hz, acetylcholine synaptic currents depressed rapidly. As previously observed (14), in response to continuous illumination, the initial peak current was followed by a high rate of asynchronous release for the entire period of illumination (Fig. 4*A Right*). It is not known whether the decrease is caused by synaptic depression or simply the inactivation of

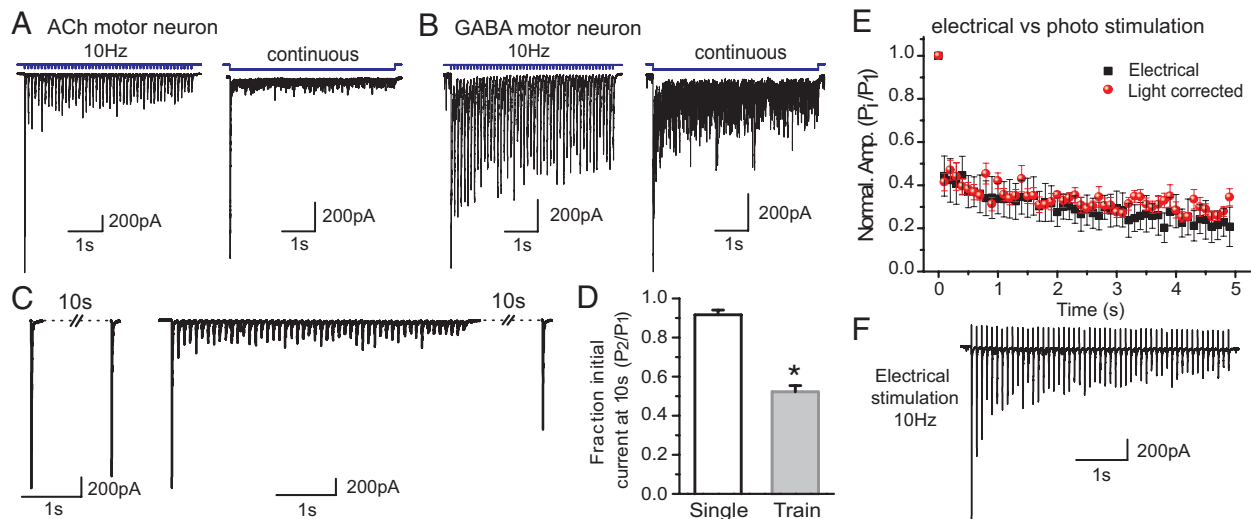


**Fig. 4.** Repetitive stimulation of postsynaptic currents. (A) Acetylcholine currents evoked by 10 Hz (Left), or a 5-s continuous (Right) light pulse in *Punc-17::ChR2::mCherry*. (B) GABA postsynaptic currents evoked by 10 Hz (Left) or a 5-s continuous (Right) light pulse in *Punc-47::ChR2::mCherry*. (C) Recovery of acetylcholine current 10 s after a single light pulse (Left) or after a 5-s train of 10 Hz light pulses (Right). (D) Recovery 10 s after a single light pulse (91.5%  $\pm$  2.2%, white column,  $n = 15$ ) or after a 10-Hz train (52.2%  $\pm$  3.2%, gray column,  $n = 23$ ;  $*P < 0.00001$ ). (E) Normalized amplitudes (to the first peak amplitude in a 10-Hz train) of evoked acetylcholine currents were plotted with time. Red spheres: light-evoked currents were corrected to the relative muscle photocurrents recorded at 10 Hz ( $n = 10$ ). Black squares: electrically evoked currents ( $n = 4$ ). (F) An example of acetylcholine currents electrically evoked by a 10-Hz train from the WT.

channelrhodopsin itself. To demonstrate that the decreased responses were caused by synaptic depression, we compared a test pulse after a single stimulus or after a high-frequency train of stimuli. The test stimulus was 10 s after the train—ample time for nearly full recovery of channelrhodopsin (96.3%; Fig. 1B). A test pulse evoked 91.5%  $\pm$  2.2% ( $n = 15$ ) of the initial response after a single conditioning light stimulus was delivered to the acetylcholine motor neurons (*Punc-17::ChR2::mCherry* animals; Fig. 4C Left and D). By contrast, a test pulse applied after 10 Hz stimulation for 5 s evoked only 52.2%  $\pm$  3.2% ( $n = 23$ ) of the first peak (Fig. 4C Right and D). These data suggest that a decrease in synaptic transmission was caused by high-frequency stimulation.

Repetitive stimulation of GABA neurons also elicited use-dependent depression of postsynaptic currents (Fig. 4B). The rate of depression was slower and the amplitudes of sustained currents were larger for GABA neurons than those for acetylcholine neurons stimulated at the same frequencies.

Some of the observed decrease in synaptic currents is a result of inactivation or a reduced conductance state of channelrhodopsin rather than synaptic depression. Channelrhodopsin photocurrents rapidly decrease and then stabilize in response to repetitive light stimuli (Fig. S2). Thus, the initial stimulating current in neurons will be of higher amplitude than subsequent stimuli. Because the synaptic responses are graded, a decrease in the stimulus strength will result in a smaller synaptic current even in the absence of synaptic depression. To measure synaptic depression, one must correct for changes in the size of the stimulus. The size of each stimulus in the neurons was linearly scaled with the light-induced current determined by direct light stimulation of *C. elegans* muscles (Fig. S2). It is possible to make this correction because the postsynaptic currents are proportional to the stimulating currents from channelrhodopsin activation (Fig. 3C). This correction is based on the assumption that channelrhodopsin currents decline in response to prolonged exposure to light in both motor neurons and muscles. This assumption is likely to be true as channelrhodopsin drops into a similar reduced conductance state in all cells tested (15, 18, 22). Nevertheless, this assumption requires validation. We can determine if our corrected measure for the rate of depression using channelrhodopsin stimulation matches the rate of depression induced by direct electrical stimulation, in which the stimulation

strength is constant. The ventral nerve cord was stimulated at 10 Hz using an electrode while recording currents in the body muscle (Fig. 4F). Only preparations exhibiting full recovery were analyzed. The normalized currents from electrically stimulated motor neurons were plotted together with the corrected values for light-stimulated postsynaptic currents (Fig. 4E). Depression determined by photo-stimulation was nearly identical to depression induced by electrical stimulation. These data demonstrate that photo-stimulation can be used to obtain measures of synaptic depression.

Acetylcholine synapses exhibit rapid depression even under low-frequency stimulation. At low-stimuli frequencies such as 0.2, 1, and 5 Hz, acetylcholine responses depressed following a single exponential decay ( $\tau = 4.71$  s  $\pm$  1.24,  $n = 7$ ; 0.58 s  $\pm$  0.11,  $n = 9$ ; and 0.09 s  $\pm$  0.02,  $n = 9$ , respectively) and eventually reached a steady state (Fig. 5A). When re-plotted against stimulus number, one can observe that depression for low-frequency stimuli depends mostly on stimulus number ( $\tau = 0.9$  stimuli  $\pm$  0.3 at 0.2 Hz,  $\tau = 0.6$  stimuli  $\pm$  0.1 at 1 Hz,  $\tau = 0.5$  stimuli  $\pm$  0.2 at 5 Hz; Fig. S44). At 1 Hz and 5 Hz, there was no further depression, and sustained transmission stabilized at approximately 50% of the initial current. At high frequencies (10 and 20 Hz), acetylcholine currents depressed at 2 rates. The very rapid rate eliminates 60%–70% of the current after a single stimulus ( $\tau = 0.2$  stimuli  $\pm$  0.3 at 10 Hz,  $n = 10$ , and 0.4 stimuli  $\pm$  0.1 at 20 Hz,  $n = 13$ ). Sustained release also depresses under high-frequency stimulation at a slower rate that is correlated somewhat better with time than stimulus number [ $\tau = 3.1$  s  $\pm$  1.8 at 10 Hz and 2.1 s  $\pm$  0.8 at 20 Hz (Fig. 5A) or  $\tau = 30.5$  stimuli  $\pm$  18.4 at 10 Hz and 42.5 stimuli  $\pm$  16.8 at 20 Hz (Fig. S44)].

What causes the rapid depression of the acetylcholine synapses? One possibility is that the receptors on the muscle desensitize to further release of acetylcholine. There are 2 types of acetylcholine receptors at the neuromuscular junction that are distinguished by their agonist sensitivities: the nicotine-sensitive and levamisole-sensitive receptors (20). These receptors exhibit distinct desensitization kinetics that can be independently observed in mutants expressing only a single receptor type. The levamisole receptor is absent in *unc-38* mutants, and the nicotine receptor is absent in *acr-16* mutants (20, 29, 30). We measured the desensitization time course of the nicotine or levamisole receptors in the continuous presence of acetylcholine (100  $\mu$ M, 5 s; Fig. 5C). Nicotine receptors

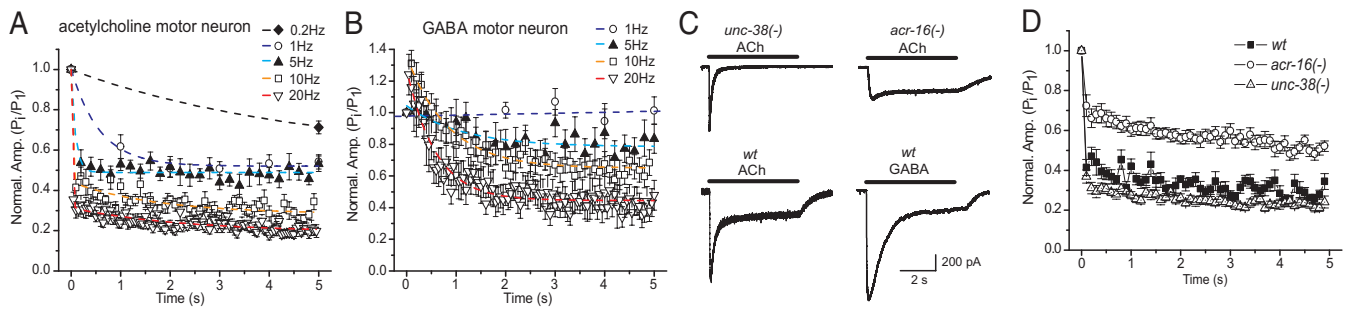


**Fig. 5.** Synaptic plasticity of acetylcholine and GABA synapses. (A) Corrected light-evoked acetylcholine currents were plotted with time at variable stimulation frequencies. Depression rates at low stimuli frequencies were best fit by single-exponential functions (0.2 Hz:  $\tau = 4.71 \pm 1.24$ ,  $n = 7$ ; 1 Hz:  $\tau = 0.58 \pm 0.11$ ,  $n = 9$ ; 5 Hz:  $\tau = 0.09 \pm 0.02$ ,  $n = 9$ ). Depression rates at high stimuli frequencies were best fit by double-exponential functions (10 Hz:  $\tau_{fast} = 0.02 \pm 0.03$ ,  $\tau_{slow} = 3.05 \pm 1.84$ ,  $n = 10$ ; 20 Hz:  $\tau_{fast} = 0.02 \pm 0.01$ ,  $\tau_{slow} = 2.12 \pm 0.84$ ,  $n = 13$ ). (B) Corrected light-evoked GABA currents were plotted with time at variable stimulation frequencies. Stimuli at 1 Hz did not cause depression (dark blue line, linear fit,  $n = 8$ ). Depression caused by 5 Hz light stimuli was best fit by a single-exponential function ( $\tau = 1.13 \pm 0.47$ ,  $n = 8$ ). Depressions following the initial facilitation at 10 Hz and 20 Hz light stimuli were fit by single-exponential decay (10 Hz:  $\tau = 0.83 \pm 0.14$ ,  $n = 13$ ; 20 Hz:  $\tau = 0.62 \pm 0.08$ ,  $n = 9$ ). (C) Exogenous acetylcholine or GABA evoked currents. (D) Corrected light-evoked acetylcholine currents depress differently in *unc-38(-)* ( $n = 18$ ) or *acr-16(-)* animals ( $n = 14$ ).

exhibit rapid and complete desensitization ( $\tau = 0.29 \text{ s} \pm 0.03$ ,  $n = 10$ ) whereas levamisole receptors exhibit little desensitization ( $79.0\% \pm 2.7\%$  initial current at 5 s,  $\tau = 1.15 \text{ s} \pm 0.14$ ,  $n = 7$ ). To investigate postsynaptic contributions to synaptic depression, we stimulated the acetylcholine neurons and measured synaptic depression in *unc-38(-)* or in *acr-16(-)* animals. Under 10 Hz stimulation, initial rates of depression of synapses containing only the nicotine receptor are more rapid than in the WT, whereas depression of synapses containing just the levamisole receptor is slower than in the WT (Fig. 5D). Slow rates of depression remain unchanged in these mutants. These data suggest that rapid depression at acetylcholine synapses is caused partially by the rapid desensitization of nicotine receptors, and slow depression is likely a result of a presynaptic mechanism.

The GABA receptors are also known to desensitize to sustained application of neurotransmitter (31). We measured desensitization of the GABA receptor by applying GABA (100  $\mu\text{M}$ , 5 s) to muscles. The rate of desensitization of GABA-induced currents ( $\tau = 0.62 \text{ s} \pm 0.10$ ,  $n = 7$ ) resembles desensitization of acetylcholine currents in the WT, i.e., when both the nicotine and levamisole receptors are present ( $\tau = 0.44 \text{ s} \pm 0.13$ ,  $n = 12$ ; Fig. 5C). These data suggested that GABA synapses would exhibit synaptic depression under high-frequency stimulation. In fact, after the first few stimuli, GABA synaptic currents exhibited an intermediate rate of depression under high-frequency stimulation (10 Hz:  $\tau = 0.83 \text{ s} \pm 0.14$ ,  $n = 13$ ; 20 Hz:  $\tau = 0.62 \text{ s} \pm 0.08$ ,  $n = 9$ ; Fig. 5B). However, GABA synaptic currents exhibited significant facilitation for the first few responses at 10 Hz and 20 Hz stimulation, and exhibited no or only slight depression at 1 Hz and 5 Hz stimulation (1 Hz: linear responses,  $n = 8$ , 5 Hz:  $\tau = 1.13 \text{ s} \pm 0.47$ ,  $n = 8$ ; Fig. 5B and Fig. S4B). These data suggest that the receptor field cannot be fully saturated with neurotransmitter and desensitized even after several evoked responses. Facilitation followed by slow depression is typical of synapses with a low probability of release (32). Thus, the facilitation of GABA currents is possibly caused by presynaptic mechanisms. Importantly, under high-frequency stimulation, both acetylcholine and GABA synapses can sustain a sizable evoked response without further depression.

## Discussion

Graded synapses exhibit several common features: tonic release of neurotransmitter, decreases or increases in release in response to hyperpolarization or depolarization, and evoked responses that are graded with respect to the size of the depolarizing stimulus. Here we demonstrate that the neuromuscular junctions of *C. elegans* exhibit the properties of graded synapses. If

channelrhodopsin were specifically localized to synapses, photo-stimulation could act locally to stimulate the synaptic calcium channels and induce graded neurotransmitter release. However, channelrhodopsin is not localized exclusively at synapses, but is rather diffuse in neurons. Moreover, photo-stimulation of the neurons elicits responses identical to electrical stimulation to distal regions of acetylcholine neurons. Thus, the graded responses observed using photo-stimulation are likely to result from passive propagation of membrane potentials into synaptic varicosities, which then cause a proportionally scaled release of neurotransmitter.

Ribbon synapses in the visual pathway possess similar properties (33–36). The presynaptic stimulus pattern is reproduced in the postsynaptic neurons due to the near linear relationships between membrane potential, calcium current, and exocytosis (4, 37). Two factors are believed to contribute to this graded synaptic transmission. First, the relationship between the rate of fusion and local calcium is relatively shallow at the ribbon synapse at low concentrations of calcium (4), so increasing calcium leads to a gradual increase in exocytosis. Most other well studied synapses exhibit an approximately third-order relationship (38–40), so increasing calcium over a small range can lead to a burst of exocytosis. Second, intracellular calcium concentrations in ribbon synapses do not increase to levels at which calcium becomes cooperative under physiological conditions (41). The underlying molecular mechanism for this specialized transmission of analog signals is still unknown (3). Nevertheless, graded synaptic transmissions grant the vertebrate ribbon synapse the extraordinary ability to relay detailed and temporally precise information about graded changes in presynaptic membrane potential. It is not clear why the nematode neuromuscular junction resembles the vertebrate visual system. One possibility is that tonic acetylcholine release maintains body-wall muscle tension, and graded release permits the body curvature or bending frequency to be precisely modulated by subtle changes in presynaptic inputs.

At most synapses, periods of elevated activity lead to use-dependent synaptic depression (42), whereas others are stable or exhibit facilitation (43, 44). Acetylcholine motor neurons in *C. elegans* exhibit conspicuous depression even after a single stimulation. About half of this rapid depression is contributed by desensitization of the postsynaptic receptor. Depletion of the presynaptic vesicle pool may contribute to slow components of depression. However, we cannot exclude contributions from nonsynaptic changes in presynaptic motor neurons. For example, because of the small diameter of *C. elegans* motor neurons, repetitive stimulation could cause changes in the ion gradients

and decrease stimulation efficiency, perhaps exacerbated by the presence of channelrhodopsin in the membrane. Nevertheless, the near-perfect overlap of depression induced by channelrhodopsin or by stimulating electrodes suggests that the mechanisms of depression are similar.

In contrast to acetylcholine synapses, GABA synapses exhibit facilitation under high frequency stimulation, followed by slow depression. Facilitation and slow depression are the hallmarks of synapses with a low release probability for the readily releasable pool (32). One must be cautious, because poor expression of channelrhodopsin might fail to activate rapid depression. However, observations of single evoked responses indicate the GABA synapses differ in a fundamental way: the presence of multiple peaks in a single evoked response suggests that asynchronous release contributes to the breadth of GABA-gated evoked currents.

One of the goals of studies of *C. elegans* is to understand how circuits produce behavior. Knowing the connectivity and whether a synapse is excitatory or inhibitory will not suffice.

- Katz B, Miledi R (1967) Tetrodotoxin and neuromuscular transmission. *Proc R Soc Lond B Biol Sci* 167:8–22.
- Llinas R, Steinberg IZ, Walton K (1981) Relationship between presynaptic calcium current and postsynaptic potential in squid giant synapse. *Biophys J* 33:323–351.
- Heidelberger R (2007) Mechanisms of tonic, graded release: lessons from the vertebrate photoreceptor. *J Physiol* 585:663–667.
- Thoreson WB, Rabl K, Townes-Anderson E, Heidelberger R (2004) A highly Ca<sup>2+</sup>-sensitive pool of vesicles contributes to linearity at the rod photoreceptor ribbon synapse. *Neuron* 42:595–605.
- Burrone J, Lagnado L (2000) Synaptic depression and the kinetics of exocytosis in retinal bipolar cells. *J Neurosci* 20:568–578.
- von Gersdorff H, Matthews G (1997) Depletion and replenishment of vesicle pools at a ribbon-type synaptic terminal. *J Neurosci* 17:1919–1927.
- Delcastillo J, Demello WC, Morales T (1963) The physiological role of acetylcholine in the neuromuscular system of *Ascaris lumbricoides*. *Arch Int Physiol Biochim* 71:741–757.
- Davis RE, Stretton AO (1989) Signaling properties of *Ascaris* motoneurons: graded active responses, graded synaptic transmission, and tonic transmitter release. *J Neurosci* 9:415–425.
- Davis RE, Stretton AO (1989) Passive membrane properties of motoneurons and their role in long-distance signaling in the nematode. *Ascaris J Neurosci* 9:403–414.
- Bargmann CI (1998) Neurobiology of the *Caenorhabditis elegans* genome. *Science* 282:2028–2033.
- Goodman MB, Hall DH, Avery L, Lockery SR (1998) Active currents regulate sensitivity and dynamic range in *C. elegans* neurons. *Neuron* 20:763–772.
- Mellem JE, Brockie PJ, Madsen DM, Maricq AV (2008) Action potentials contribute to neuronal signaling in *C. elegans*. *Nat Neurosci* 11:865–867.
- Lockery SR, Goodman MB (2009) The quest for action potentials in *C. elegans* neurons hits a plateau. *Nat Neurosci* 12:377–378.
- Liewald JF, et al. (2008) Optogenetic analysis of synaptic function. *Nat Methods* 5:895–902.
- Nagel G, et al. (2003) Channelrhodopsin-2, a directly light-gated cation-selective membrane channel. *Proc Natl Acad Sci USA* 100:13940–13945.
- Boyden ES, Zhang F, Bamberg E, Nagel G, Deisseroth K (2005) Millisecond-timescale, genetically targeted optical control of neural activity. *Nat Neurosci* 8:1263–1268.
- Han X, Boyden ES (2007) Multiple-color optical activation, silencing, and desynchronization of neural activity, with single-spike temporal resolution. *PLoS ONE* 2:e299.
- Nagel G, et al. (2005) Light activation of channelrhodopsin-2 in excitable cells of *Caenorhabditis elegans* triggers rapid behavioral responses. *Curr Biol* 15:2279–2284.
- Zhang F, et al. (2007) Multimodal fast optical interrogation of neural circuitry. *Nature* 446:633–639.
- Richmond JE, Jorgensen EM (1999) One GABA and two acetylcholine receptors function at the *C. elegans* neuromuscular junction. *Nat Neurosci* 2:791–797.
- Schuske KR, et al. (2003) Endophilin is required for synaptic vesicle endocytosis by localizing synaptotagmin. *Neuron* 40:749–762.
- Bamann C, Kirsch T, Nagel G, Bamberg E (2008) Spectral characteristics of the photocycle of channelrhodopsin-2 and its implication for channel function. *J Mol Biol* 375:686–694.
- Kohn RE, et al. (2000) Expression of multiple UNC-13 proteins in the *Caenorhabditis elegans* nervous system. *Mol Biol Cell* 11:3441–3452.
- Maruyama IN, Brenner S (1991) A phorbol ester/diacylglycerol-binding protein encoded by the *unc-13* gene of *Caenorhabditis elegans*. *Proc Natl Acad Sci USA* 88:5729–5733.
- Richmond JE, Davis WS, Jorgensen EM (1999) UNC-13 is required for synaptic vesicle fusion in *C. elegans*. *Nat Neurosci* 2:959–964.
- Francis MM, Maricq AV (2006) Electrophysiological analysis of neuronal and muscle function in *C. elegans*. *Methods Mol Biol* 351:175–192.
- Liu Q, et al. (2005) Presynaptic ryanodine receptors are required for normal quantal size at the *Caenorhabditis elegans* neuromuscular junction. *J Neurosci* 25:6745–6754.
- Juusola M, French AS, Uusitalo RO, Weckstrom M (1996) Information processing by graded-potential transmission through tonically active synapses. *Trends Neurosci* 19:292–297.
- Francis MM, et al. (2005) The Ror receptor tyrosine kinase CAM-1 is required for ACR-16-mediated synaptic transmission at the *C. elegans* neuromuscular junction. *Neuron* 46:581–599.
- Touroutine D, et al. (2005) *acr-16* encodes an essential subunit of the levamisole-resistant nicotinic receptor at the *Caenorhabditis elegans* neuromuscular junction. *J Biol Chem* 280:27013–27021.
- Bamber BA, Richmond JE, Otto JF, Jorgensen EM (2005) The composition of the GABA receptor at the *Caenorhabditis elegans* neuromuscular junction. *Br J Pharmacol* 144:502–509.
- Dobrunz LE, Stevens CF (1997) Heterogeneity of release probability, facilitation, and depletion at central synapses. *Neuron* 18:995–1008.
- Naka KI, Itoh MA, Chappell RL (1987) Dynamics of turtle cones. *J Gen Physiol* 89:321–337.
- Sakai HM, Naka K (1987) Signal transmission in the catfish retina. V. Sensitivity and circuit. *J Neurophysiol* 58:1329–1350.
- Tranchina D, Gordon J, Shapley R, Toyoda J (1981) Linear information processing in the retina: a study of horizontal cell responses. *Proc Natl Acad Sci USA* 78:6540–6542.
- Wu SM (1985) Synaptic transmission from rods to bipolar cells in the tiger salamander retina. *Proc Natl Acad Sci USA* 82:3944–3947.
- Rabl K, Cadetti L, Thoreson WB (2006) Paired-pulse depression at photoreceptor synapses. *J Neurosci* 26:2555–2563.
- Borst JG, Sakmann B (1999) Effect of changes in action potential shape on calcium currents and transmitter release in a calyx-type synapse of the rat auditory brainstem. *Philos Trans R Soc Lond B Biol Sci* 354:347–355.
- Mintz IM, Sabatini BL, Regehr WG (1995) Calcium control of transmitter release at a cerebellar synapse. *Neuron* 15:675–688.
- Wu LG, Westenbroek RE, Borst JG, Catterall WA, Sakmann B (1999) Calcium channel types with distinct presynaptic localization couple differentially to transmitter release in single calyx-type synapses. *J Neurosci* 19:726–736.
- Rieke F, Schwartz EA (1996) Asynchronous transmitter release: control of exocytosis and endocytosis at the salamander rod synapse. *J Physiol* 493:1–8.
- Zucker RS, Regehr WG (2002) Short-term synaptic plasticity. *Annu Rev Physiol* 64:355–405.
- Martin AR, Pilar G (1964) Presynaptic and post-synaptic events during post-tetanic potentiation and facilitation in the avian ciliary ganglion. *J Physiol* 175:17–30.
- Wang LY, Kaczmarek LK (1998) High-frequency firing helps replenish the readily releasable pool of synaptic vesicles. *Nature* 394:384–388.

Graded release suggests that the output of a circuit may be a shifting integration of analog inputs. Moreover, use-dependent plasticity will change the character of synapses during behavior. Modeling behavior must move beyond arithmetic.

## Materials and Methods

A detailed description of methods is in *SI Text*.

**Electrophysiology.** Electrophysiological methods were performed as previously described (20, 27) with minor adjustments. Light source was an AttoArc 2 HBO 100-W system. A Zeiss bandpass filter set was used to excite channelrhodopsin (at 450–490 nm) or halorhodopsin (at 540–552 nm). The light on/off switch was controlled by a Uniblitz VS25 shutter.

**ACKNOWLEDGMENTS.** We thank Alexander Gottschalk, Ed Boyden, and Marc Hammarlund for reagents. We thank V. Maricq, M. Ailion, M. Palfreyman, and C. Frøkjær-Jensen for comments on this manuscript. This work was supported by the Howard Hughes Medical Institute (E.J.) and by National Institutes of Health Grant NS034307 (to E.J.) and the Jane Coffin Childs postdoctoral fellowship funded by HHMI (to G.H.).

# Supporting Information

Liu et al. 10.1073/pnas.0903570106

**Plasmids.** DNA sequence encoding the amino-terminal 314 aa of channelrhodopsin, excluding the initiating methionine, was amplified by PCR using the plasmid *Pmyo-3::ChR2(gf)::YFP* (gift from Alexander Gottschalk, Goethe University, Frankfurt, Germany) as template for primers GGGGACAAGTTTGTACAAA-AAAGCAGGCTCCGATTATGGAGGCGCCCTGAGTGCCG and GGGGACCACTTTGTACAAGAAAGCTGGGTACTTG-CCGGTGCCTTGTGACCGCGCCAGCCTCGGCC. This introduced flanking *attB* recombination sites, and the resulting amplification product was recombined with pDONR 221 (Invitrogen) using BP Clonase II (Invitrogen) to produce the *attL1/attL2*-containing entry clone pGH39. A minigene encoding mCherry with worm-optimized codons and 3 artificial introns (gift from Karen Oegema, University of California, San Diego) was amplified with primers (GTTTGGATCCGCTCAAAGGGTGAAGAAGTAAC and CAAAAGTCTTATACAATTATCCATGC-CAC) that include 5' BamHI and 3' SpeI restriction sites. The PCR product was digested with these enzymes and ligated into the small multiple cloning sites in front of the *unc-54UTR* in pMH472 (gift from Marc Hammarlund, Yale University, New Haven, CT). The resulting *attR2/attL3*-containing entry clone (pGH38) translationally fuses mCherry onto the carboxy terminus of channelrhodopsin when recombined with pGH39 in a Multisite Gateway LR reaction (Invitrogen). The promoter of *unc-17* was amplified from EcoRV-linearized RM348p (gift from Jim Rand, University of Oklahoma, Oklahoma City) with GGGGACAACCTTGTATAGAAAAGTTGTACACCAATCATTTCTCCCCTCC and GGGGACTGCTTTTTTGTACAAACTTGCCATTTTGAACAAGAGATGCGGAAAATAGAAAG for subsequent recombination with pDONR P4-P1R (Invitrogen) to produce the *attL4/attR1*-containing entry clone pGH1. The *unc-47* promoter was amplified using GGGGACAACCTTTGTATAGAAAAGTTGACTAACTTCTACGTCAAAAAGTTGAC and GGGGACTGCTTTTTTGTACAAACTTGTCATCTGTAATGAAATAAATGTGACGCT before the creation of pMH522 (gift from Marc Hammarlund) by BP recombination with pDONR P4-P1R. The *myo-3* promoter in a Gateway entry vector was from Open Biosystems (p\_K12F2.1.93). To drive expression of ChR2::mCherry in body wall muscles, cholinergic neurons, or GABA neurons, one of the 3 promoter entry clones was re-combined with pGH38, pGH39, and the destination vector pDEST R4-R3 (Invitrogen) using LR Clonase Plus (Invitrogen). The resulting expression clones are *Pmyo-3::ChR2::mCherry::unc-54UTR* (pGH15), *Punc-17::ChR2::mCherry::unc-54UTR* (pGH57) and *Punc-47::ChR2::mCherry::unc-54UTR* (pGH58).

DNA sequence encoding halorhodopsin (gift from Ed Boyden, MIT, Cambridge, MA), excluding the initiating methionine, was amplified with GGGGACAAGTTTGTACAAAAGCAGGCTTGACTGAGACCTCCACCCG and GGGGACCACTTTGTACAAGAAAGCTGGGTAGTCATCGGCAGGTGTG-CCG. This *attB1/2* flanked amplification product was recombined with pDONR 221 using BP Clonase II to produce entry clone pGH48. A minigene encoding GFP(65C) with 3 artificial introns (gift from Chris Richie, National Institutes of Health, Bethesda, MD) was amplified with primers that included 5' BamHI and 3' SpeI restriction sites. The PCR product was digested and ligated in front of the *unc-54UTR* in pMH472 (gift from Marc Hammarlund, Yale University, New Haven, CT). The resulting *attR2/attL3*-containing entry clone (pGH50) translationally fuses GFP onto the carboxy terminus of halorhodopsin when re-combined with pGH48 in a Multisite Gateway LR reaction. *Punc-17::Halo::GFP::*

*unc-54UTR* (pGH52) and *Punc-47::Halo::GFP::unc-54UTR* (pGH51) were made by recombination with pGH1 and pMH522, respectively.

**Strains.** EG5027 *oxIs353 [Pmyo-3::ChR2::mCherry::unc-54UTR lin-15(+)] V* was made by x-ray bombardment of EG4549 *lin-15(n765ts) X; oxEx973*. The extrachromosomal array was made by injecting MT1642 *lin-15(n765ts)* with 30 ng/uL pGH15 and 70 ng/uL *lin-15* rescuing plasmid pL15EK (2).

EG5096 *oxIs364 [Punc-17::ChR2::mCherry::unc-54UTR lin-15(+)] LITMUS 38i] X* and EG5182 *oxIs407 [Punc-17::ChR2::mCherry lin-15(+)] Litmus38i] X* were made by x-ray bombardment of EG4811 *lin-15(n765ts) X; oxEx1086*. The extrachromosomal array was made by injecting MT1642 *lin-15(n765ts)* with 33 ng/uL each of pGH57, pL15EK, and LITMUS 38i (NEB).

EG5025 *oxIs351 [Punc-47::ChR2::mCherry::unc-54UTR lin-15(+)] LITMUS 38i] X* and EG5026 *oxIs352 [Punc-47::ChR2::mCherry::unc-54UTR lin-15(+)] LITMUS 38i] IV* were made by x-ray bombardment of EG4812 *lin-15(n765ts) X; oxEx1087*. The extrachromosomal array was made by injecting MT1642 *lin-15(n765ts)* with 33 ng/uL each of pGH58, pL15EK, and LITMUS 38i (NEB).

EG4813 *lin-15(n765ts) X; oxEx1088 [Punc-17::Halo::GFP::unc-54UTR lin-15(+)] LITMUS 38i] X* was made by injecting MT1642 *lin-15(n765ts)* with 33 ng/uL each of pGH52, pL15EK, and LITMUS 38i (NEB).

EG4814 *lin-15(n765ts) X; oxEx1089 [Punc-47::Halo::GFP::unc-54UTR lin-15(+)] LITMUS 38i] X* was made by injecting MT1642 *lin-15(n765ts)* with 33 ng/uL each of pGH51, pL15EK, and LITMUS 38i (NEB).

All the listed integrants were out-crossed and mapped for use in this study. EG5183 *unc-13(s69) I; oxIs364 [Punc-17::ChR2::mCherry::unc-54UTR lin-15(+)] LITMUS 38i] X* was made by crossing EG5096 with BC168 *unc-13(s69) I*. EG5548 *unc-38(x20) I; oxIs407 [Punc-17::ChR2::mCherry lin-15(+)] Litmus38i] X* was made by crossing EG5182 with ZZ20 *unc-38(x20) I*. EG5546 *acr-16(ok789) V; oxIs364 [Punc-17::ChR2::mCherry lin-15(+)] Litmus38i] X* was made by crossing EG5096 with RB918 *acr-16(ok789)*. EG5547 *acr-16(ok789) V; oxIs407 [Punc-17::ChR2::mCherry lin-15(+)] Litmus38i] X* was made by crossing EG5182 with RB918 *acr-16(ok789)*.

All strains were maintained at 22 °C on standard nematode growth medium seeded with OP50. WT is Bristol N2. Other strains used in this study are ZZ20: *unc-38(x20)I*, VM4006 (10X outcross of RB918) *acr-16(ok789) V*.

**Electrophysiology.** Electrophysiological methods were performed as previously described (3, 4) with minor adjustments. All preparations subjected to repetitive stimulation recovered peak current amplitudes after approximately 1 min of rest. Briefly, animals were immobilized in cyanoacrylate glue (Vetbond tissue adhesive; 3M), and after a lateral incision was made in the dorsolateral region, the cuticle flap was folded back and glued down (Nexaband; Abbott Animal Health) to expose the ventral body wall muscles. The preparation was then treated with collagenase (type IV; Sigma) for approximately 15 s at a concentration of 0.5 mg/mL. Borosilicate glass pipettes (BF100–58–10; Sutter Instruments) with a tip resistance of approximately 3–5 M $\Omega$  were used as electrodes for voltage clamping. A medial muscle on the right side of the nerve cord was then voltage-clamped using the whole-cell configuration at a holding potential

of -60 mV. All recordings were made at room temperature (22 °C) using an EPC-10 patch-clamp amplifier (HEKA). Data were acquired using Patchmaster software (HEKA). All data analysis and graph preparation was performed using Fitmaster (HEKA), Mini Analysis (Synaptosoft), and OriginPro 7.5 (Origin Lab). All statistic data are presented as mean  $\pm$  SEM.

**Recording Solutions.** The extracellular solution contained: 150 mM NaCl, 5 mM KCl, 5 mM CaCl<sub>2</sub>, 1 mM MgCl<sub>2</sub>, 10 mM glucose, 5 mM sucrose, 15 mM Hepes, pH 7.35, OSM  $\approx$ 340 mOsm. The standard pipette solution contained: 120 mM KCl, 20 mM KOH, 4 mM MgCl<sub>2</sub>, 5 mM N-Tris hydroxymethyl methyl-2-aminoethane-sulfonic acid (TES), 0.25 mM CaCl<sub>2</sub>, 4 mM NaATP, 36 mM sucrose, 5 mM EGTA, pH 7.2, OSM  $\approx$ 320 mOsm. Under these conditions, GABA release generates inward currents as a result of high chloride concentrations in the intracellular solution (4). Equilibrium-chloride intracellular solutions for recording of acetylcholine currents contained: 113 mM K gluconate, 7 mM KCl, 20 mM KOH, 4 mM MgCl<sub>2</sub>, 5 mM N-Tris hydroxymethyl methyl-2-aminoethane-sulfonic acid, 0.25 mM CaCl<sub>2</sub>, 4 mM NaATP, 36 mM sucrose, 5 mM EGTA, pH 7.2, OSM  $\approx$ 320 mOsm.

**Electrical Stimulation.** Electrically evoked responses were elicited using a electrode with a tip resistance of approximately 3–5 M $\Omega$  positioned along the ventral nerve cord approximately 1 muscle cell body length away from the patched muscle. A square wave depolarizing current of 0.5 ms at 25 V was delivered from an SIU5 stimulation isolation unit driven by an S48 stimulator (Grass Telefactor).

**Pressure Ejection.** Acetylcholine or GABA (Sigma) was dissolved in extracellular solution to a final concentration of 100  $\mu$ M and filled into a pipette of 2–3 M $\Omega$  tip resistance. Pressure ejection (4 psi, 5 s) was controlled by a valve (Valve Driver II; General Valve) triggered by EPC-10 (HEKA).

**Paired-Pulse Protocol.** For each trial, we first gave a single pulse that was followed by a second pulse after a variable delay. These inter-pulse intervals ranged from 50 ms to 15 s. Between consecutive trials there was  $>$ 30 s of darkness to allow for

complete channel recovery. We determined the ratio of the second current peak to the first current peak, and plotted these ratios relative to the recovery intervals.

**Illumination System.** Light source was from an AttoArc 2 HBO 100W system (Zeiss) with an Osram mercury arc bulb (Osram). A Zeiss bandpass filter set was used to excite channelrhodopsin (at 450–490 nm) or halorhodopsin (at 540–552 nm). Light intensity was controlled by dialing the power supply. Light on/off switch was controlled by a VS25 shutter and a VCM-D1 driver (Uniblitz). Light-activated currents in channelrhodopsin or halorhodopsin transgenic animals were evoked by shining light (10 mW/mm<sup>2</sup> unless specified) onto the dissected worm preparation on a Zeiss Axioskop microscope, equipped with a  $\times$ 40 water-immersion objective and  $\times$ 15 eyepieces. Rapid shutter opening and closing was triggered by TTL signals from the HEKA EPC-10 amplifier. A liquid light guide (Sutter) was installed between the Axioskop microscope and the shutter to avoid mechanical vibrations during repetitive stimulations. Light intensity was measured with a Coherent FieldMax II-TOP laser power/energy meter.

**Retinal Feeding.** Transgenic worms were grown in the presence of all-trans retinal approximately 16–48 h before electrophysiological experiments. All transRetinal (Sigma) was dissolved in ethanol to make 100 mM stock solution and stored at -20 °C in the dark. Nematode growth medium plates were seeded with 4  $\mu$ L 100 mM retinal stock solution mixed with 250  $\mu$ L OP50 per 50-mm plate. Seeded retinal plates were kept in the dark at -4 °C for as long as 1 week. Young adult transgenic worms were transferred from regular plates to freshly seeded retinal plates in the dark at room temperature

**Fluorescence Microscopy.** Worms are immobilized by using 2% phenoxy propanol and imaged on a Pascal LSM5 confocal microscope with Zeiss Plan-Apochromat 63  $\times$  1.4NA oil objectives.

**Data Fitting.** Single exponential function was fit by the equation:  $y = A_1 \exp(-x/\tau_1) + y_0$ . Double exponential function was fit by the equation:  $y = A_1 \exp(-x/\tau_1) + A_2 \exp(-x/\tau_2) + y_0$ .

1. White JG, Southgate E, Thomson JN, Brenner S (1976) The structure of the ventral nerve cord of *Caenorhabditis elegans*. *Philos Trans R Soc Lond B Biol Sci* 275:327–348.
2. Clark SG, Lu X, Horvitz HR (1994) The *Caenorhabditis elegans* locus *lin-15*, a negative regulator of a tyrosine kinase signaling pathway, encodes two different proteins. *Genetics* 137:987–997.

3. Liu Q, et al. (2005) Presynaptic ryanodine receptors are required for normal quantal size at the *Caenorhabditis elegans* neuromuscular junction. *J Neurosci* 25:6745–6754.
4. Richmond JE, Jorgensen EM (1999) One GABA and two acetylcholine receptors function at the *C. elegans* neuromuscular junction. *Nat Neurosci* 2:791–797.

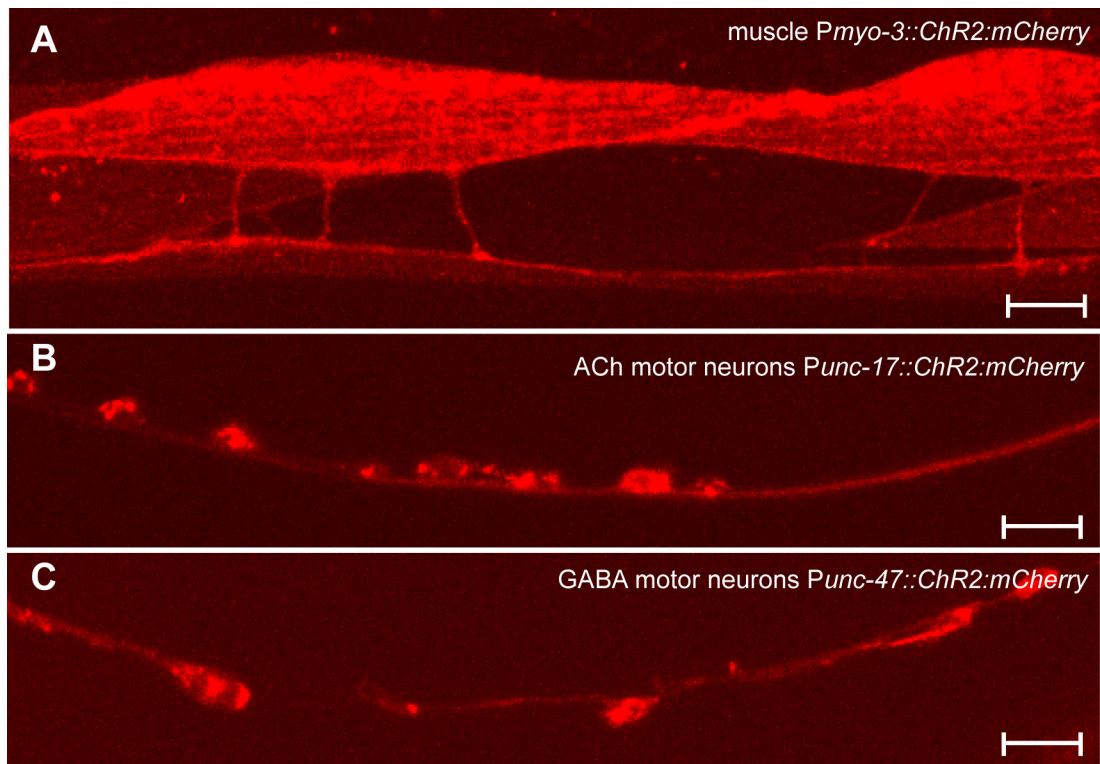


**Fig. S1.** Expression of channelrhodopsin in *C. elegans*. (A) Expression of *Pmyo-3::ChR2::mCherry* in *C. elegans* body wall muscles. (B) Expression of *Punc-17::ChR2::mCherry* in *C. elegans* acetylcholine motor neurons. (C) Expression of *Punc-47::ChR2::mCherry* in *C. elegans* GABA motor neurons. (Scale bar: 10  $\mu\text{m}$ .)

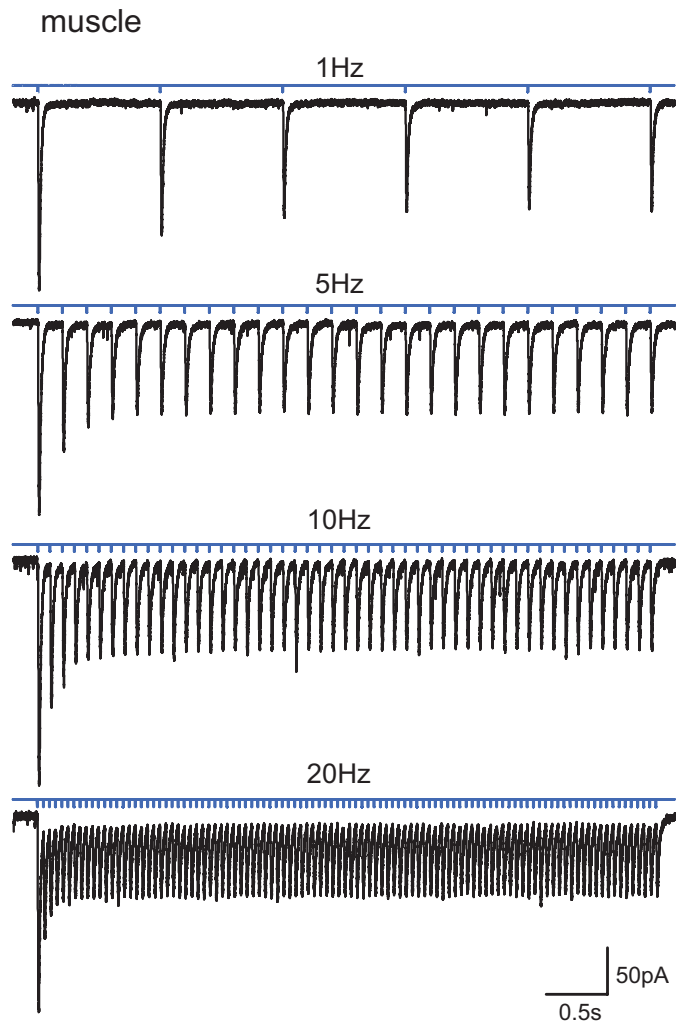


**Fig. S2.** Channelrhodopsin-induced photocurrents in muscle. Examples of photocurrents activated by trains of 3-ms light stimuli at frequencies of 1, 5, 10, or 20 Hz, respectively.



